



Universitat Ramon Llull

DOCTORAL THESIS

Title TAILORING SURFACES TO IMPROVE BIOMATERIALS
PERFORMANCE: piCVD & iCVD APPROCHES

Presented by Laura Montero Suarez

Centre Institut Químic de Sarrià

Departament Enginyeria Industrial

Directed by Dr. Salvador Borrós

*A mis padres,
porque siempre me habéis apoyado*

¿Qué sería de la vida, si no tuviéramos el valor de intentar algo nuevo?

Vincent Van Gogh

Acknowledgements

Primer de tot m'agradaria donar-li les gràcies al meu director de tesi, Dr. Salvador Borrós. Chicho moltes gràcies per confiar tant en mi, per deixar-me viure tantes experiències durant aquests anys i per donar-me l'oportunitat de fer una estada a Boston. Gràcies per haver-me convençut (com tu dius) per fer la tesi i sobretot per creure que tot això era possible!

M'agradaria agrair a l'IQS, la concessió de la beca de doctorat que ha permès realitzar aquesta feina durant 3 anys.

I would like to thank Prof. Karen K. Gleason. Thanks for giving me a chance to work in your group. I appreciate your guidance and confidence in me throughout the year I spent in your lab. Thanks for the great teaching! Special thanks to Dr. Salmaan Baxamusa. Thank you for showing me around in my year at MIT, teach me so many things and discuss with me all the results in our research, it was AWESOME!

També m'agradaria agrair a la Dra. Rosa Villa, la Dra. Gemma Gabriel i l'Antón Guimerà del CNM, la seva col·laboració en el projecte dels hidrogels per recobrir els sensors d'impedància. Moltes gràcies pel coneixement i per la tecnologia compartida.

A tot el grup GEMAT!! Gràcies per ajudar-me en tot moment! Sou moltes persones les que heu format part d'aquesta petita família i que heu estat al meu costat durant aquests 4 anys, des de que vaig marxar a Boston i m'aguantàveu per telèfon, gràcies Berta V., Jose i Núria M. i després aquests últims anys tots els que m'heu recolzat dia a dia. Núria A., gràcies per acollir-nos quan entrem al grup i acompanyar-nos tot el camí. ElenITA, gracias por ser un pilar indispensable de GEMAT, Nat gracias por ser tan inocente, Pri por esas conversaciones sin fin,

Oscar per la paciència amb els bitxus. Joan et quedes el títol de Mr. Reactor, fes honor del nom que és molt important!! Abdón gràcies per tota la feina que has fet aquest últim any, semblava que no ens en sortiríem però com diu el Chicho, he de confiar més! Maria gràcies per dir les coses com son, he après molt al teu costat, Maaaaajoooo por estar ahí, dentro y fuera del IQS, me has entendido con solo mirarme y me has hecho reír cuando lo he necesitado. Aniiiiii gràcies per les tardes de reactor interminables, les classes particulars de química, per les xerrades infinites, les sortides en bici.... Victor, mmggrraaaa, no cal dir gaire més, gràcies per aconsellar-me i per fer-me creure una miqueta més en les coses, aiiixx quina paciència! Mariona tu també ets part d'aquesta tesi, t'estimo infinit! I en definitiva, gràcies a tot el grup!

No em vull oblidar de les nenes, moltes gràcies per estar al meu costat sempre! Sou les millors del món! Em fa molta il·lusió poder dir que hem crescut, i que seguirem creixent juntes, sou part de la meva família i us estimo moltíssim! David creo que has sufrido la peor parte de un doctorado (y lo has aguantado mejor que yo), gracias por ayudarme, por hacerme reír, por entenderme y distraerme, por pasar tiempo conmigo y sobre todo por estar a mi lado siempre. Ha sido genial compartir este trocito de camino a tu lado ☺.

Por último quiero agradecerse a mi familia, que siempre me han demostrado lo mucho que me querían y lo orgullosos que estaban de mi, a mis abuelos (a los cuatro) os quiero muchísimo. Y sobre todo a mis padres porque siempre han confiado en mí, porque nunca habéis dudado que conseguiría llegar a este punto y porque me habéis apoyado y querido muchísimo. Gracias por hacerme las cosas mucho más fácil.

A tots vosaltres, MIL GRÀCIES!!!!

Summary (English)

Tailoring Surfaces to improve Biomaterials performance:

piCVD & iCVD approaches

Thin hydrogel films have been deposited to modify surface properties and improve biomaterials performance. Two of the most common chemical vapor deposition techniques have been studied to carry out these modifications. Photo-initiated chemical vapor deposition piCVD has been developed as a simple, not aggressive and easy method for the deposition of thin hydrogel films. This method follows a versatile surface-driven reaction process that allows homogeneous coating of both 2D and 3D geometries, such as microspheres. piCVD offers the possibility to fabricate a wide range of swellable thin films, incorporating co-monomers with different properties, such as amine-reactivity, suitable for further modification. The hydrogels can be designed by nano-confining the reactivity to the near surface region, improving the chemical functionality of hydrogels. In addition, a new method to create micro-patterned surfaces can be applied during piCVD deposition to design surfaces having special behavior.

Thermo-responsive thin hydrogel films have also been obtained via initiated chemical vapor deposition (iCVD). A library of thermo-sensitive films exhibiting controlled lower critical solution temperatures (LCST) has been generated. Quartz crystal microbalance with dissipation analysis has been used to analyze the phase-transition of these films. The intrinsic properties of thermo-sensitive hydrogels, such as tunable surface hydrophilicity or release of film-entrapped molecules, open the possibility to design systems for controlling biofilm formation.

Sumari (Català)

Tailoring Surfaces to improve Biomaterials performance:

piCVD & iCVD approaches

S'han dipositat capes primes d'hidrogeles per tal de modificar les propietats superficials i millorar el comportament dels biomaterials. Dues de les tècniques de deposició química en fase vapor més comunes s'han estudiat per poder dur a terme aquestes modificacions. La deposició química foto-iniciada en fase vapor (piCVD) és un mètode simple, ràpid i no agressiu que permet depositar films d'hidrogeles. És un mètode que s'inicia a la superfície de la mostra i que permet recobrir de manera homogènia superfícies tridimensionals com és el cas de les micro-partícules. El piCVD ofereix un ventall molt ampli d'hidrogels amb capacitat d'absorbir aigua, incorporant co-monomers amb diferents propietats. Els hidrogels poden ser dissenyats perquè la reactivitat es localitzi a nivell superficial, millorant d'aquesta manera la funcionalització química dels hidrogels. Tanmateix, un nou mètode s'ha utilitzat per micro-estructurar les superfícies durant la deposició via piCVD per obtenir hidrogels amb comportaments especials.

Els hidrogels termo-sensibles s'han obtingut via deposició química iniciada en fase vapor (iCVD). S'ha desenvolupat una llibreria d'hidrogels termo-sensibles, els quals exhibeixen una temperatura de transició molt marcada. La microbalança de quars amb dissipació (QCM-D) s'ha fet servir per analitzar la transició d'aquests films. La combinació de les propietats que ofereixen els films termo-sensibles dona la possibilitat de dissenyar una plataforma per prevenir la formació de biofilms.

Table of contents

Summary (English)	V
Sumari (Català)	VI
Table of contents	VII
Index of Figures	X
Index of Tables	XIV
Index of Equations	XIV
Acronyms List	XV
Chapter 1. <i>Introduction</i>	1
Chapter 2. <i>Photoinitiated Chemical Vapor Deposition of Hydrogel Thin Films</i>	17
2.1. <i>Introduction</i>	19
2.2. <i>Experimental Section</i>	23
2.2.1. <i>Film Synthesis. piCVD Polymerization</i>	23
2.2.2. <i>Functional Hydrogel Preparation</i>	26
2.2.3. <i>Microsphere and Sensor Modification</i>	28
2.2.4. <i>Chemical Characterization of Films</i>	29
2.2.5. <i>Swelling Characterization of Films</i>	30
2.2.6. <i>Interaction of pHEMA with Proteins</i>	31
2.2.7. <i>Depth Profile of Films Determined by ToF-SIMS</i>	31
2.2.8. <i>Surface Functionalization of Thin Film Hydrogels</i>	32
2.2.9. <i>Silica Microspheres Coated with pHEMA</i>	33
2.3. <i>Results</i>	34
2.3.1. <i>piCVD Deposition Mechanism and Chemical Structure OF pHEMA-based Hydrogels</i>	34

Table of contents

2.3.2.	Depth Profile of the PFM-functional Hydrogel	37
2.3.3.	Hydrogel Swelling Properties and Thin Film Structure	38
2.3.4.	Protein Adhesion on pHEMA Surface	46
2.3.5.	pHEMA-based Hydrogel Functionalization	48
2.3.6.	Silica Microspheres and Sensor Coated with pHEMA Thin Film	49
2.4.	Discussion	54
Chapter 3.	<i>Biofunctional Polymer Surfaces</i>	57
3.1.	Introduction	59
3.2.	Experimental Section	62
3.2.1.	Fabrication of Patterned Surfaces	62
3.2.2.	Structure Determination of Patterned Surfaces by AFM and SEM Analysis	64
3.2.3.	Surface Functionalization of the Patterned Structures	65
3.3.	Results	66
3.3.1.	Fabrication of Ordered Surfaces via Patterning Processes	66
3.3.2.	Thickness Evaluation of Film Micro-geometries	68
3.4.	Discussion	73
Chapter 4.	<i>Hydrogel Thin Film Coatings For Stable Sensor-Tissue Interface</i>	75
4.1.	Introduction	77
4.2.	Experimental Section	81
4.2.1.	Fabrication of an Impedance Sensor and its Modification with pHEMA Hydrogel	81
4.2.2.	Electrode-Electrolyte Impedance Characterization	84
4.2.3.	Mechanical Stability Test of Electrodes	85
4.2.4.	Electrode Surface Analysis	85
4.2.5.	Evaluation of Impedance Sensor Performance <i>in vivo</i>	85
4.3.	Results	87
4.3.1.	Characterization of Electrode Surfaces by SEM Analysis	87

Table of contents

4.3.2.	Electrical Characterization of Sensors	89
4.3.3.	Mechanical Characterization of Sensors	97
4.4.	Discussion	101
Chapter 5.	<i>Thermo-responsive Behavior of pNIPAAm Thin Film Hydrogels by QCM-D</i>	103
5.1.	Introduction	105
5.2.	Experimental Section.....	109
5.2.1.	Synthesis of Thermo-responsive Films via iCVD	109
5.2.2.	Thermo-responsive Surface Characterization	111
5.2.3.	Determination of LCST Temperature by QCM-D Analysis	113
5.2.4.	Bacterial Adhesion, Proliferation and Detachment on Thermo-responsive Films	115
5.2.5.	Preparation of a Control Release System based on Thermo-responsive Films	118
5.3.	Results	120
5.3.1.	Surface Characterization of Thermo-responsive Hydrogels	120
5.3.2.	Determination of the LCST Temperature via QCM-D Analysis	127
5.3.3.	Development of a Library of Thermo-responsive Hydrogels.....	129
5.3.4.	Monitoring of Bacterial Detachment upon Phase Transition	140
5.3.5.	Evaluation of the Effect on Bacterial Proliferation of a Drug Released from a Thermo-responsive	144
5.4.	Discussion	147
Chapter 6.	<i>Conclusions</i>	149
6.1.	Conclusions (English)	151
6.2.	Conclusions (Català)	154
Chapter 7.	<i>References.....</i>	157

Index of Figures

Figure 1.1. Sensoring process in a device and in a living organism	4
Figure 1.2. A) Physical immobilization B) Chemical immobilization	5
Figure 1.3. Typical representation of Cellular encapsulation.	7
Figure 1.4. HFCVD chamber	11
Figure 1.5. Reaction mechanism for iCVD polymerization.....	12
Figure 2.1. Schematic of CVD chamber	24
Figure 2.2. Schematic representation of the chemical composition and physical structure.....	27
Figure 2.3. Comparison of FTIR spectra between pHEMA standard and piCVD synthesized..	35
Figure 2.4. FTIR spectra of three co-polymer compositions.	37
Figure 2.5. ToF-SIMS depth profile of GP and HP.	38
Figure 2.6. Typical reversible swelling response of piCVD pHEMA.....	39
Figure 2.7. Swollen water content as a functional of vapor residence time.	40
Figure 2.8. Equilibrium swollen water content as a functional of fractional saturation of monomer during deposition.	41
Figure 2.9. Equilibrium swollen water content as a function of deposited thickness	42
Figure 2.10. Equilibrium swollen water content as a functional of distance between the sample and the UV lamp.....	43
Figure 2.11. Swollen water content as a function of the increasing PFM content for both the bulk and graded co-polymer.	44
Figure 2.12. Average mesh size of swollen films, as calculated by Equation 2.1.....	46
Figure 2.13. Surface nitrogen content.	47
Figure 2.14. FTIR spectra of the co-polymer synthesized by piCVD before and after the functionalization with H ₂ N-PEG-NH ₂	49

Index of Figures

Figure 2.15. Response curves of an uncoated and coated optodes.	50
Figure 2.16. SEM cross-section of a 50 μm silica microsphere coated with piCVD pHEMA.	51
Figure 2.17. SEM images of uncoated and coated 5 μm silica microspheres.	52
Figure 2.18. AFM images of uncoated and coated 800 nm silica microspheres.	52
Figure 2.19. SEM images of silica spheres using a shacking method during the deposition.	53
Figure 3.1. 3D Schematic representation of the patterning process (not to scale).	61
Figure 3.2. 2D Schematic representation of the patterning process (not to scale).	64
Figure 3.3. Top-down and oblique-angle SEM of typical patterned surface.	66
Figure 3.4. Dynamic microcondensation experiment.	67
Figure 3.5. Spatially-selective fluorescent functionalization of patterned films.	68
Figure 3.6. SEM Cross section showing topography of depressed squares.	69
Figure 3.7. AFM of the microwells in its dry state.	70
Figure 3.8. AFM of the microwells in its swollen state.	71
Figure 3.9. 3D AFM image of hydrophobic depressions in a hydrophilic matrix in its dry state (left) and swollen state (right).	72
Figure 4.1. Schematic profile of the electrode area and coating of the hydrogel.	80
Figure 4.2. Images of both impedance sensors.	82
Figure 4.3. Black platinum deposited on gold electrode surface.	87
Figure 4.4. SEM images of (a) bare electrodeposited black platinum and (b) pHEMA film.	88
Figure 4.5. SEM images taken with FIB in the electrode area to obtain cross-section profiles.	89
Figure 4.6. Evolution of the impedance modulus and phase as a function of frequency.	91
Figure 4.7. Equivalent circuit model of electrode-electrolyte interface impedance.	92
Figure 4.8. Evolution of the impedance modulus as a function of frequency.	95
Figure 4.9. Evolution of the impedance modulus as a function of frequency.	96

Index of Figures

Figure 4.10. Evolution of the impedance module at 100 Hz of sensors coated (lines) and uncoated (squares) in saline solution.	98
Figure 4.11. 10 <i>in vivo</i> experiments after getting the sensor in contact with a rabbit cornea... 99	
Figure 4.12. Picture taken in <i>in vivo</i> experiments to demonstrate the black platinum detachment for uncoated device.....	99
Figure 5.1. Schematic representation of the internal transition of thermo-responsive films..	106
Figure 5.2. Schematic result of a WCA experiment(Krüß n.d.)	112
Figure 5.3. QCM-D image. Model E1 from Q-Sense.....	113
Figure 5.4. Real-time response of (A) frequency and (B) dissipation (QSense n.d.)	114
Figure 5.5. Schematic representation of the followed protocol to test pNIPAAm surfaces.....	116
Figure 5.6. Static contact angles, below and above LCST, of different NIPAAm copolymers... 122	
Figure 5.7. WCA representation below and above LCST for three samples.	123
Figure 5.8. Static contact angles, below and above the LCST, of NIPAAm and DEAAm films... 124	
Figure 5.9. AFM images of the NIPAAm copolymers surfaces together with their roughness. 126	
Figure 5.10. 3D AFM images of NIPAAm hydrogels.	126
Figure 5.11. QCM-D graphs confirming the linear dependency of the f on temperature.	128
Figure 5.12. Representative results showing the (a) frequency and (b) dissipation for N90 hydrogel.	129
Figure 5.13. LCSTs corresponding to NIPAAm-co-EGDA thin films.	131
Figure 5.14. LCSTs corresponding to NIPAAm-co-DMAAm thin films.....	134
Figure 5.15. LCSTs corresponding to NIPAAm-co-AAc thin films.	137
Figure 5.16.LCSTs corresponding to DEAAm-co-DMAAm thin films.....	139
Figure 5.17. Percentage of cell adhesion when the temperature was decreased from 37 °C to 27 °C.....	141

Index of Figures

Figure 5.18. Percentage of cell adhesion when the temperature was increased from 27 °C to 37 °C.....	142
Figure 5.19. Adhered cells on PS (a) and NIPAAm (b).....	143
Figure 5.20. Influence of bacitracin on pNIPAAm and PS samples.....	146

Index of Tables

Table 2.1. Standard conditions for all the experimental series	25
Table 2.2. Reactor conditions for deposition of piCVD polymer films	25
Table 2.3. Experimental conditions for the co-polymer synthesis.....	27
Table 4.1. Experimental conditions for planar-sensors (series S) and micro-needles (series N).84	
Table 5.1. Experimental conditions for all the film synthesis.	111
Table 5.2. Experimental conditions for all the samples incubated.	116
Table 5.3. Modifications applied to each surface to carry out the <i>in-vitro</i> experiments.	119

Index of Equations

Equation 2.1.	45
Equation 4.1.	92
Equation 4.2.	93
Equation 5.1.	114
Equation 5.2.	118

Acronyms List

Acronyms List

AAc: Acrylic Acid

ABMP: 2,2'-azobis(2-methylpropane)

AFM: Atomic Force Microscopy

BSA: Bovine Serum Albumin

CFU: Colony Forming Unit

CPE: Constant Phase Element

CVD: Chemical Vapor Deposition

DEAAm: N,N-diethyl acrylamide

DMAAm: N,N-dimethyl acrylamide

DSC: Dual Source Column

EGDA: Ethylene Glycol

EIS: Electrochemical Impedance Spectroscopy

ESEM: Environmental Scanning Electron Microscopy

FTIR: Fourier Transform Infrared Spectroscopy

FTSC: Fluorescein-5-thiosemicarbazide

GMA: Glycidyl Methacrylate

HEMA: 2-hydroxyethyl methacrylate

HFCVD: Hot Filament Chemical Vapor Deposition

iCVD: Initiated Chemical Vapor Deposition

LCST: Lower Critical Solution Temperature

MFC: Mass Flow Controller

NIPAAm: N-isopropylacrylamide

OD: Optical Density

PECVD: Plasma Enhanced Chemical Vapor Deposition

PFA: Perfluorodecylacrylate

PFM: Pentafluorophenylmethacrylate

piCVD: Photo-Initiated Chemical Vapor Deposition

P_M: Partial pressure of the monomer

PPECVD: Pulsed Plasma Enhanced Chemical Vapor Deposition

PS: Polystyrene

P_{sat}: Saturation Pressure of the monomer

Acronyms List

QCM: Quartz-Crystal Microbalance

TEM: Transmission Electron Microscope

QCM-D: Quartz-Crystal Microbalance with
Dissipation

ToF-SIMS: Time-of-Flight Secondary Ion
Mass Spectroscopy

RCT: Charge Transfer Resistance

T_s: Substrate Temperature

RMS: Root Mean Square

TSB: Tryptic Soy Broth

sccm: Standard Cubic Centimeter per
Minute

UCST: Upper Critical Solution Temperature

SEM: Scanning Electron Microscopy

UV: Ultraviolet

WCA: Water Contact Angle

SPR: Surface Plasmon-Resonance

XPS: X-ray Photoelectron Spectroscopy

SWNT: Single-Wall NanoTube

TBPO: tert-butyl peroxide

Chapter 1.

Introduction

In design of micro-device systems, polymers are taking an important role, because they introduce additional functionality to developed surfaces and provide switchable properties. Nowadays, this kind of materials has applications ranging from sensors and actuators to drug delivery (Elman et al. 2009) and tissue engineering (J. A. Hubbell 1995), among others.

Commercially available substrates like biosensors or medical devices require the integration of a protective coating layer, because they may exhibit damages when exposed to high temperature or solvents. They present 3D structures and typically they are not biocompatible by per se. These problems among others can be solved with the design of smart surfaces.

Rapid advances in microelectronics have made available technical intelligence. There is a growing interest in the realization of systems with life-like, biomimetic or biologically inspired features (Maki K 2007). Sensors were originally designed as technical sensing organs and under this premise, it might be useful to study a living organism to adapt different parts to a sensing device. In a human being, the skin, the body's outer protective casing, receives a stimulus (e.g.: touch, noise, temp) that is transmitted to the spinal cord in the form of nerve impulses. The information transmitted initiates actions.

Figure 1.1. shows the similarities in signal acquisition and (signal) processing between a modern sensor and a living organism. In both cases, the sensing process can be separated into three basic operations. First of all, both in a living organism and in a sensor, the receptor is required to be in direct contact with the environment. The information is transformed into an electrical signal and transmitted to the processing unit (i.e.: a microcomputer or the central nervous systems), which evaluates the signal (Gründler 2007).

A key factor in the fabrication of sensors is the quality of the coupling between the receptor and the physical transducer, which responds to environmental parameters by changing some of its inherent properties. The performance of sensors is highly sensitive to the techniques used to couple these two components; this aspect is often called “interfacial design”.

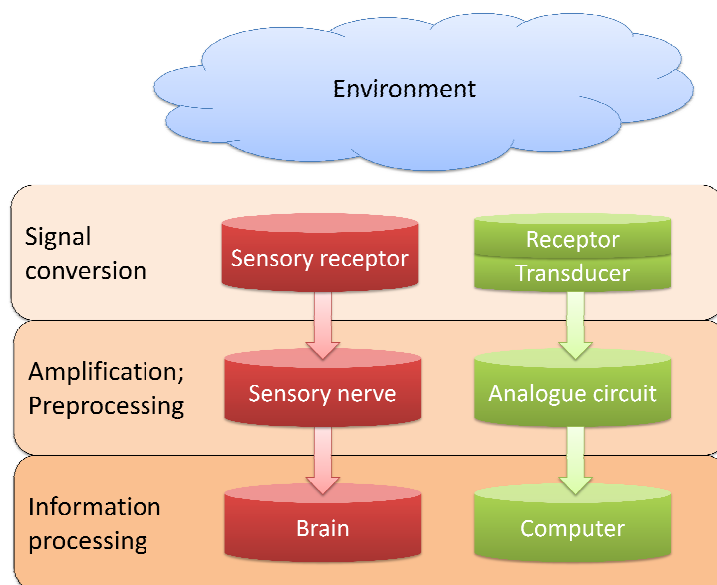


Figure 1.1. Sensing process in a device and in a living organism

Consequently, a sensor detects target analytes in the presence of interfering substances by coupling a receptor with a physical device that translates the information (concentration of target analyte) into light, heat, mass, among others. It is possible to estimate the concentration of analyte by changing this quality to an electrical signal using a physical transducer that can be electrodes, thermistors, quartz crystal microbalances (QCMs) or semiconductor devices (Rajinder S 1994; Muguruma 2007).

The receptor is made by immobilizing biomaterials and related materials, for example, enzyme and polymer (Tsai et al. 2005). The methods for sensing an analyte on a membrane are classified as chemical or physical. Chemical methods involve the formation of chemical bond

between functional groups on the support material and the analyte (Byfield & Abuknesha 1994). The functional groups are generally chosen from biological substances as enzymes, antibodies, DNA's, receptors, tissues and microorganisms because of their excellent selective functionality for target substances.

Physical immobilization methods do not involve the formation of covalent bonds with the analyte, so the native composition of the analyte remains unaltered. Physical immobilization methods are roughly classified as adsorption, entrapment, and encapsulation methods. An entrapment method is where the analyte is trapped in the interstitial spaces in the polymer matrix to be detected. Figure 1.2. shows schematically the immobilization methods.

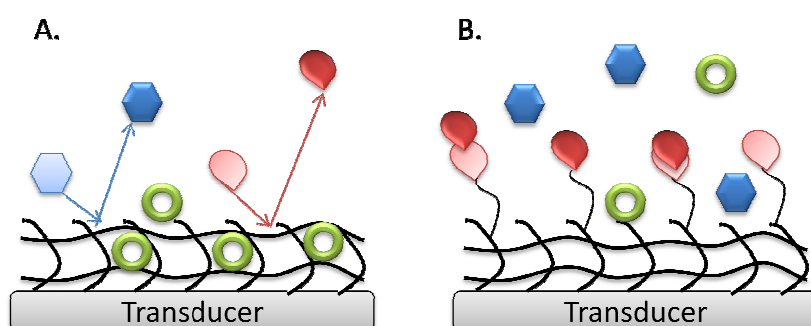


Figure 1.2. A) Physical immobilization B) Chemical immobilization

In order to address this twofold immobilization having a tunable behavior depending on the characteristics of the analyte as well as the transducer, hydrogel films have been developed.

Hydrogel thin films appear as potential candidates for sensing applications since they match all the structural requirements. Hydrogels are polymer networks that have the capability of absorbing large amounts of water without dissolving.(Peppas et al. 1985; Abraham et al. 2005) They made of cross-linked polymeric structures containing either covalent bonds produced by

the reaction of one or more co-monomers, physical cross-links from chain entanglements, association bonds such as hydrogen bonds or Van der Waals interactions between chains (Peppas & Brannon-Peppas 1990). These coatings provide an additional mechanical buffer layer between the sensing device and the biological media, resulting in excellent protective layer. Another advantage is that various bioactive reagents, such as growth factors or anti-inflammatory drugs can be embedded in the hydrogel coatings for *in situ* or *in vivo* sensing applications (Johnson et al. 2005; Y. Y. Li et al. 2003; Slowing et al. 2007).

Materials with hydrogel-like properties are generally considered to favor biocompatibility, because they are able to achieve similar water content to human tissue, providing a bio-friendly environment, and as a result, have gained strong acceptance in bioengineering (K. Y. Lee et al. 2004; Bures et al. 2001; Peppas et al. 2000). Coatings made of these water swellable and flexible materials mask the underlying surfaces and create a network, where water-soluble analytes can diffuse through the matrix. The cross-link density of the hydrogel can control the degree of diffusion as the interstitial space of the polymer network. Example of poly(2-hydroxyethyl methacrylate) (pHEMA) was one of the first hydrogels that was studied for biological applications was poly(2-hydroxyethyl methacrylate) (pHEMA), which has been extensively explored in medical uses, ranging from contact lenses (Peppas & Yang 1981; Ng & Tighe 1976) to research on artificial corneas and neural tissue engineering.

The details of the interfacial contact between the device and the tissue are important not only for promoting cell adhesion, but also for facilitating the transport of the analyte to the device. In general, biosensors are inadequate for long-term implantation, because cellular encapsulation plays a significant role in limiting the access of the analyte to the sensing receptor. Figure 1.3. shows schematically how increase the encapsulation in a device in a

biological environment . The key to success lies in developing active surfaces that improve the differences in mechanical properties, bioactivity, and mechanisms of charge transport between the engineered electronic device and the biological environment

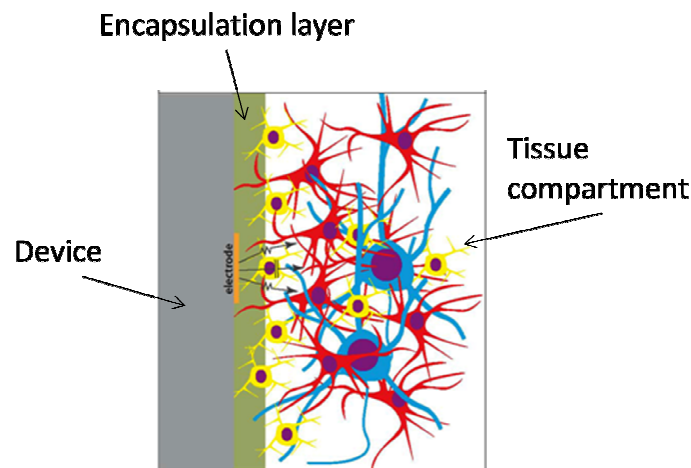


Figure 1.3. Typical representation of Cellular encapsulation.

As protein and cellular encapsulation increase, the device communication decreases because current paths become smaller (Shain 2012)

Stimuli-responsive polymers are a type of hydrogels that exhibit properties that can change in response to external stimuli such pH, light, temperature, electric or magnetic fields, among others. Relative to their extensive use, they also play a pivotal role in field of biofouling and biocompatibility.

The term biofouling is defined as the accumulation of proteins, cells and other biological materials on a surface (J. A. Hubbell 1995). Biofouling processes may decrease the performance of sensing devices by hampering the diffusion of target analytes to the sensing receptor, resulting in inaccurate measurements. In addition, most implanted medical devices frequently encounter a sequence of host defense mechanisms, such as acute and chronic

inflammation, wound healing processes and foreign body responses that may also reduce the diffusion of the analyte and the decrease in sensor response. The body response to an implant reduces the diffusion of the analyte and the decrease in sensor response. The lack of stability after implantation and the limited biosensor lifetime are the reasons why the use of biosensors is restricted to several hours or to one-use.

Another important limitation in the long-term implantation of biosensors and other medical devices is the tendency to rapidly accumulate colonizing organisms, mainly bacteria and pathogenic fungi (von Eiff et al. 2005). The adhesion of microorganisms on the surfaces of implanted sensors is of crucial importance, because, once adhered, microorganisms form colonies and subsequently complex biofilms, which may lead to foreign body-related infections (FBRIs). And this is the first step for the development of an infection (Von Recum & Jacobi 1999; James M 1993).

It is possible to overcome these limitations by modifying the surface of the biosensor with this kind of hydrogel or stimuli-responsive polymers. The most known strategy is to develop a film having chemical reactivity, which allows the immobilization of specific moieties, such as products to reduce bacterial adhesion, or materials with antifouling properties to prevent unspecific protein deposition and subsequently cell adhesion. Another possibility is to design the surface topology to confer specific antifouling and biocidal features (Wisniewski & Reichert 2000). Receptor composition, including micro-architecture of the surfaces has been related to membrane performance in vivo. It has been suggested that textured rather than smooth surfaces could lead to improved sensor performance.

Many techniques have been developed to produce thin films hydrogels. Typical preparations of thin films are wet processes or dry processes. The prominent methods of polymer wet

depositions are solution phase grafting (Zubaidi & Hirotsu 1996), casting from polymer solution (Folkman & Moscona 1978; M. Feng 1996) or confined solution phase polymerization (Chilkoti et al. 1993):

- Solution phase grafting requires a graftable surface. It is a two-step process involving the creation of radicals or suitable functional group on the surface followed by graft polymerization.
- Casting requires the solubilization of the polymer in a suitable solvent and needs a post-treatment to create cross-links.
- Confined solution phase polymerization is able to create a cross-linked polymer thin film in one polymerization step, but this technique requires a number of solution preparation steps and subsequent confinement of the solution to produce a thin film.

All these techniques allow film formation of different cross-link densities by preparing solutions of different compositions. The main disadvantages of these approaches are that the chemical structures and the properties of the polymers are independent of the actual monomer. In addition, it is a time-consuming process and has poor thickness control and lack of topology.

In contrast to these wet techniques, dry processes present environmental benefits by limiting the use of solvents and avoiding potential retention of solvents in the films which is known to be related with biocompatibility problems. Thus, processes that avoid solvents and high temperatures are desired for the synthesis of conformal coatings of stimuli-response hydrogels on substrates of various geometries. The most popular dry method of polymer thin film deposition is Chemical Vapor Deposition (CVD).

CVD is able to produce polymers on substrates *in situ* from their monomeric building blocks without the use of solvents. CVD can be used to deposit polymers for which no practical solvent exists. In addition, thickness control is excellent, as films are grown *in situ* and it is able to produce films of nanoscale thickness on a wide variety of substrates with macroscale uniformity. Uniform coatings on complex geometries can be prepared (Pierson 1999), because surface-tension effects associated with wet methods are non-existent for CVD.

CVD is a chemical process that involves chemical reactions; therefore an energy input is usually required to initiate the polymerization. The parameter that differentiates one CVD technique from another is the type of energy input, also giving the technique's name.

In Hot Filament CVD (HFCVD) (Mao & Gleason 2004; Lewis et al. 2001) technique, the use of thermal energy allows selective chemistries to occur inside the chamber, so that only certain chemical reactions are favored. The use of this technique allows the growth of polymeric films that are spectroscopically indistinguishable from polymers obtained by conventional polymerization techniques (Lau et al. 2003). The resistively-heated wires in HFCVD heat the gas but not the substrate, which is backside-cooled to promote adsorption of monomeric species. The thermal breakdown of species creates radicals responsible for film growth. As seen in Figure 1.4, an HFCVD chamber is similar to an ordinary CVD chamber, except that a filament array is suspended above the substrate. The filament temperature and the total power input are important HFCVD parameters that require appropriate control to obtain high quality films.

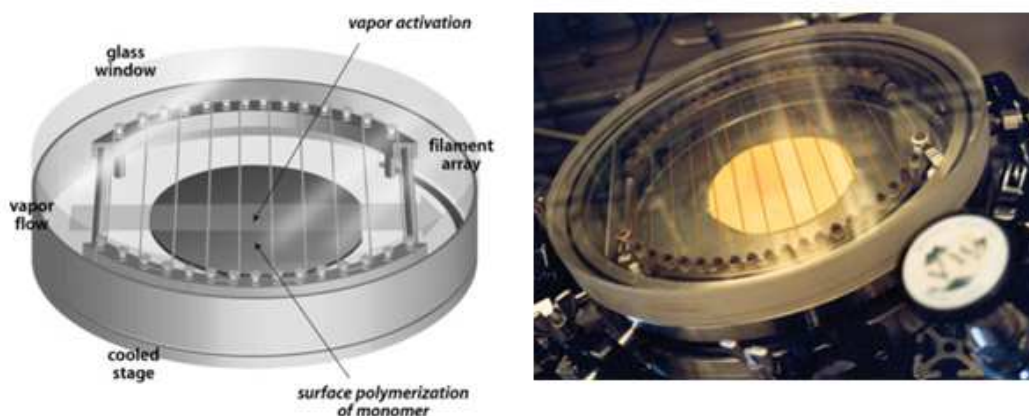
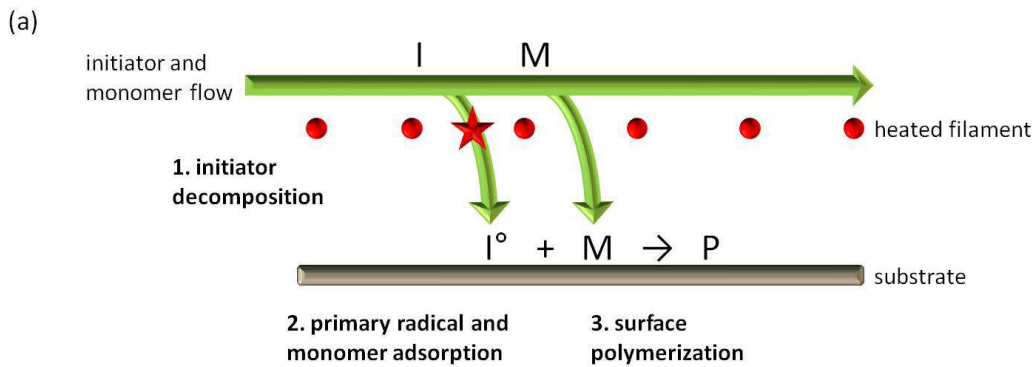


Figure 1.4. HFCVD chamber

The initiated CVD (iCVD) (Lau & Gleason 2006; Chan & Gleason 2005b; Chan & Gleason 2005a; O'Shaughnessy et al. 2007) method is a subset of hot filament CVD (HFCVD), in which selective thermal decomposition of species is achieved using resistively-heated filament wires. Mainly, the use of an initiator in iCVD techniques improves the capability of producing structurally well-defined polymer films, when compared to HFCVD. Similarly to the initiators used in traditional free-radical polymerization, the initiators in iCVD are thermally-labile species that are fragmented in order to create radicals. Mao and Gleason have demonstrated the possibility to use iCVD to polymerize different (meth)acrylic monomers, such as iCVD of a methacrylic polymer from the same family as pHEMA: poly(glycidyl methacrylate) (pGMA). In this work, glycidyl methacrylate (GMA) and tert-butyl peroxide (TBPO) were used as the monomer and the initiator, respectively. Due to the low bond-dissociation energy of the peroxide bond in TBPO, low filament temperatures (180 – 250 °C) are required to generate radicals for initiation. As a result of low temperatures, the bond-scission chemistry inside the chamber is limited to only the fragmentation of TBPO. These radicals act as initiators of polymers chains to which multiple monomer units are subsequently added in a chain propagation-like manner. The use of an initiator not only allows superior control of the film

chemistry, but also accelerates film growth.(Mao & Gleason 2004; Lewis et al. 2001; S. K. Murthy et al. 2002)

As outlined in Figure 1.5, the reaction mechanism proposed for iCVD polymerization can be explained in three reaction steps. The proper polymerization is started by the initiator radicals, which attack the vinyl groups of the monomers. Next, the initiator radicals and the monomers diffuse and adsorb from the vapor phase onto the substrate. At the last stage, growth of the polymer chain is terminated.



(b)

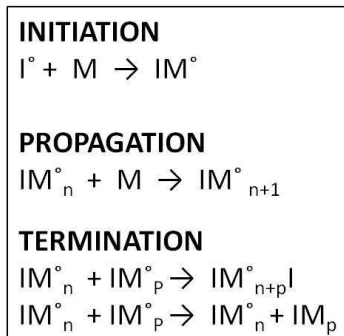


Figure 1.5. Reaction mechanism for iCVD polymerization.

(a) scheme of the three reaction steps (b) Free radical polymerization steps (Lau & Gleason 2006)

Chapter 1 - Introduction

Photo-initiated CVD (piCVD) is an evolutionary CVD technique for depositing polymeric thin films in one step without using heat activation. The technique requires no pre- or post-treatment and usually a volatile photoinitiator is used to initiate free-radical polymerization of gaseous monomers under ultraviolet (UV) irradiation. The vapors are fed into a vacuum chamber in which film growth is observed on a substrate exposed to UV irradiation. The resulting thin films are comprised of linear chains and have high structural resemblance to conventionally-polymerized polymers (Chan & Gleason 2005a).

Aims

The aim of this thesis is to investigate the capability of piCVD and iCVD techniques as a platform to improve the interface between biodevices and living tissues. Thin film hydrogels are presented as a promising solution to enhance the mentioned interface. These structures must face different problems, as it has been stated before, because they are in contact with a complex biological environment and must guarantee the proper working of the device.

Different surface modifications are presented to improve biosensor's performance. The techniques and microstructures that are achieved show a wide range of possibilities in the field of bio-MEMS.

First, the evaluation of piCVD process takes place to investigate the capability of the technique and at the same time understanding the deposition mechanism. It intends to broaden the horizon of the method from homopolymers to different applications. Chapter 2 investigates the structure and properties of the films, and evaluates the hydrogel as protective coating for optical sensors in biological environments. In addition, the analysis of a chemical functional molecule is done to compare the difference into the film. A co-monomer is added in a graded fashion way, where the functionality will be confined only to the surface, the other possibility is to obtain a bulk co-polymerization.

The study of the impact of the surfaces' design is performed in different structures. The architecture design and manufacture of surfaces with potential effects in bacterial adhesion contributes towards a better understanding of the performance. The interactions with patterns and randomize surfaces are described in Chapter 3, the effects of the surface

roughness, the wettability and the changes in topography induced by the stimuli responsive hydrogels.

Chapter 2 and Chapter 3 open up the possibilities of using these thin hydrogel films as protective layers for biosensors in *in vivo* applications. Chapter 4 aims to validate the potential of these techniques in a real *in vivo* application by preventing signal degradation in sensitivity and response time.

The last part of this thesis was centered in the study of the iCVD techniques to develop temperature responsive hydrogels. Chapter 5 allows characterization of temperature-responsive hydrogels and monitors the temperature-driven changes in the hydrogel state. Thermo-responsive hydrogels offer the opportunity to develop a new interface between bio-device and media that may contain microorganism.

Chapter 2.

Photoinitiated Chemical Vapor Deposition of Hydrogel Thin Films

Originally published as:

S.H. Baxamusa, L. Montero, J.M. Dubach, H.A. Clark, S. Borros, K.K. Gleason, *Biomacromolecules* **2008**, 9 (10), pp 2857-2862

L. Montero, S.H. Baxamusa, S. Borros, K.K. Gleason, *Chemistry of Materials* **2009**, 21 (2), pp 399-403

2.1. Introduction

The first step in this thesis was to study the technique that would allow developing a stable interface between sensing device and biological media. This chapter reports photoinitiated chemical vapor deposition (piCVD), a gentle synthetic method for the preparation of ultrathin films (~100 nm) of the hydrogel poly(2-hydroxyethyl methacrylate) (pHEMA). The technique deposits a selectively permeable coating with a mesh size large enough to allow small molecule analytes to permeate the film, but small enough to prevent the transport of large biomolecules, such as proteins. The absence of solvents and plasmas allows films to be directly synthesized on sensors without degradation of interfering sensitivity or response time.

The modification of surfaces to enhance their compatibility with biological media, both *in vivo* and *in vitro*, is of great interest for applications ranging from biomedical implants (Yamine et al. 2005; Adden et al. 2006) to tissue engineering (Discher et al. 2005; Stevens & George 2005; Hirano & Mooney 2004). Surface modification is also critical for sensing applications (Lou et al. 2006; Gavalas et al. 2006; Wisniewski & Reichert 2000), with particular focus on the potential of an *in vivo* glucose sensor to assist in the treatment of diabetic individuals (Quinn et al. 1997). However, any sensor that is to come in contact with biological media, including *in vivo* implants, must be compatible with the physiological environment. Chief among compatibility concerns is the ability of a surface to resist non-specific protein adhesion, to prevent both biofouling on the device surface as well as inflammation and thrombosis (Gorbet & Sefton 2004). Biologically relevant sensing devices represent a unique challenge in this regard, because any surface modification that reduces non-specific protein adhesion must still allow the passage of the analytes of interest (Quinn et al. 1997). Additionally, the surface modification process must not degrade the functionality of the device (Wisniewski & Reichert

2000). The attachment of long polymer brushes is a common method for enhancing the biocompatibility of surfaces (Satomi et al. 2007; Waku et al. 2007; R. Murthy et al. 2007), but these methods require chemical modification of the surface that can degrade the sensor function. Thin polymer films that are not covalently attached are another common modification (Emr & Yacynych 1995), but the solvents used in their preparation can degrade devices, particularly enzymatic biosensors (Wisniewski & Reichert 2000; Quinn et al. 1997). The hydrogel poly(2-hydroxyethyl methacrylate) (pHEMA) has been deposited on different substrates via a solvent-free plasma process (G. P. Lopez et al. 1993), but never directly on a sensor. pHEMA has been used extensively in biological and biomedical applications (G. P. Lopez et al. 1993; Corkhill et al. 1989; Chirila et al. 1993), and its biocompatibility, including resistance to protein adhesion (Tanaka et al. 2001; Bajpai & Kankane 2008; Morra & Cassinelli 1995), has been investigated. When synthesized as a cross-linked network, pHEMA films have small mesh sizes that prevent the permeation of large biomolecules (Peppas et al. 1985).

For sensors designed for biological applications or physiological implantation, the development of a solvent-and plasma-free method for the synthesis of stable, swellable, cross-linked hydrogel thin films is highly desirable because the energetic species present in the glow discharge are deleterious to the device. Here, the photoinitiated chemical vapor deposition (piCVD) of ultrathin pHEMA films with tunable cross-link densities is presented.

Hydrogels have been modified by many available chemistries and techniques to incorporate functional groups (Bures et al. 2001; Elbert & J. A. Hubbell 1996; W. Chen & McCarthy 1997; J. a Hubbell 1999; Ikada 1994; Siow et al. 2006; Yu et al. 2005). Because of the limited ability of large molecules such as proteins or other biologically relevant ligands to diffuse into polymers, functional groups at the surface react most readily. In contrast, unreacted functional groups

within the hydrogel matrix are problematic, because they can negatively impact bulk properties and generate undesired reactions, particularly over long time scales (C. L. Feng et al. 2005). Thus, some research groups have centered their attention on changing only the near-surface properties of hydrogel films.

The current work seeks to achieve homogeneous and graded functional group incorporation into hydrogel thin films using the one-step technique of piCVD. The functional co-monomer pentafluorophenyl methacrylate (PFM) is co-polymerized with HEMA by piCVD. It should be noted that the solubility contrast of the hydrophilic HEMA monomer and the hydrophobic PFM monomer makes this co-polymer difficult to achieve via solution phase techniques. Previous work demonstrated that the PFM group can be successfully incorporated into films by plasma enhanced CVD (Francesch et al. 2005) and initiated CVD (O'Shaughnessy et al. 2007). Since the PFM ester is reactive towards amino groups (Francesch et al. 2007), the incorporation of PFM results in a versatile platform for subsequent functionalization with a multitude of amine-containing compounds.

Polymers with homogenous incorporation of functional groups, here termed "bulk" co-polymers, are synthesized by maintaining constant flow rates of both HEMA and PFM throughout the course of the deposition. The strategy for achieving graded layers in which PFM is confined to the near surface region (~20 nm) is to flow the PFM monomer into the CVD reactor only during the final period of growth. The continuity in growth with the first pure HEMA (99+%) layers creates a gradient in functional group incorporation without the need for physically stacking chemically dissimilar layers.

The bulk co-polymer, the graded co-polymer, and the pure HEMA films could be compared, providing insight into the importance of functional group distribution on reactivity and

physico-chemical properties. Graded functional layers via piCVD offer several potential benefits. First is the ability to independently control bulk film properties, like swellability and modulus, and surface reactivity. Second is the elimination of functional groups in the bulk of the film, which have limited ability to react and can be detrimental to the bulk film properties. Finally, graded films enable the use of lesser amounts of expensive functional monomer.

The polymerization is initiated by exposing monomer vapors under moderate vacuum to low power density ultraviolet light. This method is similar to iCVD, a dry process that has been used to synthesize a variety of polymers as thin films (Martin et al. 2008; Lau & Gleason 2008; Tenhaeff & Gleason 2008). No solvent or plasma is used, the polymerization occurs near room temperature (20-40 °C), and the hydrogel can be synthesized on virtually any surface. The films synthesized are cross-linked during the deposition, and the cross-link density allows for the passage of water and small molecule analytes, while preventing the transport of macromolecules such as proteins. The films are stable in aqueous media and more resistant to non-specific protein adhesion than bare silicon. Since sensors for the detection of physiologically significant analytes are often fabricated in particulate form (Clark et al. 1999; Vollmer et al. 2002), it is also demonstrated that microparticles can be easily and conformally coated. It could be interesting to demonstrate that the piCVD synthesis is gentle enough to coat a delicate optode sensor without degrading its response to its target analyte, sodium.

2.2. Experimental Section

2.2.1. Film Synthesis. piCVD Polymerization

Different experimental series were conducted to characterize piCVD as a method for the preparation of ultrathin films of the hydrogel pHEMA for the protection of sensors in biological applications.

Polymer films were deposited on 100 mm diameter silicon (Si) substrates in a custom-built vacuum reactor. The reactor had a cylindrical shape with a height of 33 mm and a radius of 120 mm. The inlet of precursor gases and the exhaust were placed at opposite ends of the reactor. The top of the reactor was covered by a removable quartz plate (125 mm radius and 25 mm thickness), allowing visual inspection, laser interferometry, and appropriate placement of the substrate. The chamber pressure was maintained constant by a throttling butterfly valve (Model 653B, MKS), and the substrate temperature (T_s) was controlled via backside contact of the deposition stage with temperature-controlled water lines. The clearance between the stage and the quartz plate was 33 mm. A laser interferometer (633 nm He-Ne laser source JDS Uniphase) allowed real time tracking of the deposited film thickness and termination of film growth at the desired film thickness.

To run a piCVD experiment, a low-power ultraviolet lamp (Model UVG-54, UVP) was mounted above the reactor to initiate the polymerization. The lamp emits ultraviolet light at 254 nm wavelength. The quartz viewport allowed the light to enter the chamber. HEMA monomer (99+%) was used as received without any additional purification. The liquid monomer was vaporized in a stainless steel jar and its vapor was metered into the reactor through a MFC (Model 1152, MKS). No separate photoinitiator was used.

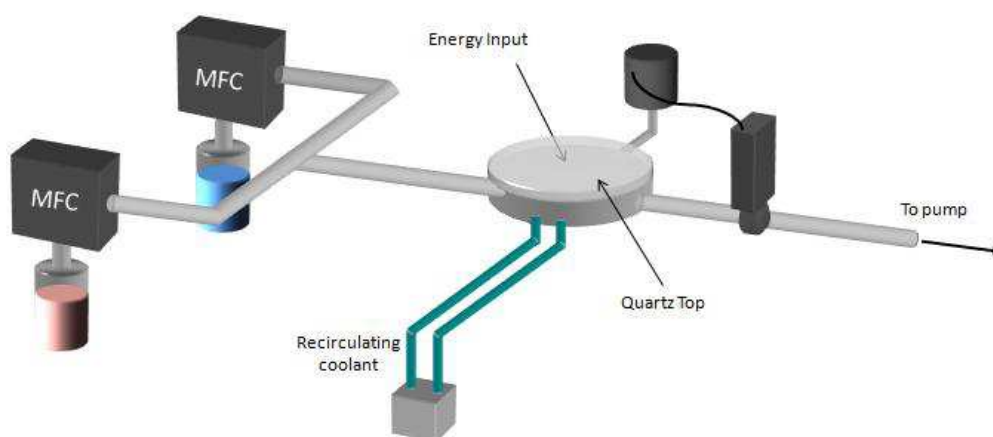


Figure 2.1. Schematic of CVD chamber

In order to identify the driving polymerization mechanism, two experimental settings were performed. The first set of experiments was designed to investigate the effect of main free path of molecules in the vapor phase (experimental series A) and the second one was designed to evaluate the effect of temperature stage (experimental series B). All films in experimental series A and B were approximately 200 nm thick and deposited on flat silicon wafers. Deposition rates varied between 1 - 40 nm/min, depending on the operating conditions.

In addition, experimental series C and experimental series D were proposed, in order to evaluate the influence on the final polymer of the thickness and the distance between the UV lamp and the sample.

For each piCVD run, experimental parameters were maintained constant (as summarized in Table 2.1.), except one, which was varied according to the experimental series (A, B, C or D). The swelling properties of the resulting pHEMA films were evaluated. Analysis of the experimental data revealed that the degree of swelling decreased with increasing cross-linking density.

Table 2.1. Standard conditions for all the experimental series

HEMA flow (sccm)	Temperature stage (°C)	Pressure (mTorr)	Lamp-Sample Gap (inch)	UV wavelength (nm)
2.0	30	100	3 ½	254

Operating conditions of the piCVD experimental series analyzed in this work are shown in the following table.

Table 2.2. Reactor conditions for deposition of piCVD polymer films

Sample Name	HEMA Flow (sccm)	Temperature stage (°C)	Gap (inch)	Thickness (nm)
A1	1.0	30	3 ½	200
A2	1.5	30	3 ½	200
A3	2.0	30	3 ½	200
A4	2.5	30	3 ½	200
B1	2.0	20	3 ½	200
B2	2.0	25	3 ½	200
B3	2.0	30	3 ½	200
B4	2.0	40	3 ½	200
C1	2.0	30	3 ½	100
C2	2.0	30	3 ½	200
C3	2.0	30	3 ½	300
C4	2.0	30	3 ½	400

Sample Name	HEMA Flow (sccm)	Temperature stage (°C)	Gap (inch)	Thickness (nm)
D1	2.0	30	0	200
D2	2.0	30	1 ½	200
D3	2.0	30	3 ½	200
D4	2.0	30	6 ¼	200
D5	2.0	30	10 ¼	200

2.2.2. Functional Hydrogel Preparation

The piCVD process and reactor have been described in detail previously in 2.2.1. All samples were deposited on silicon wafers maintained at 30 °C through backside coolant circulation. PFM (97%, Monomer Polymer) and HEMA (99+%, Sigma) monomers were used as received without further purification. HEMA was heated to 80 °C in a temperature-controlled crucible and its vapors were metered into the reactor through a mass flow controller (MKS, 1152). The flow rate of PFM, which was heated to 60 °C in a separate crucible, was also metered with a mass flow controller. A throttling butterfly valve (MKS, 653B) was used to control the pressure inside the chamber. The film growth was initiated by exposing the substrate to 50 $\mu\text{W}\cdot\text{cm}^{-2}$ ultraviolet light of 254 nm wavelength. Film growth was monitored *in situ* with the use of an interferometer (JDS Uniphase, 1508) to obtain the desired film thickness.

Two types of films were deposited in this work: bulk co-polymers and graded co-polymers. For the bulk co-polymers (experimental series H), both monomers, HEMA and PFM, were introduced into the reactor simultaneously during the polymerization. The HEMA flow rate was kept constant for all the bulk co-polymer depositions, while the PFM flow rate was systematically varied between samples. The reactor pressure was varied for each deposition to

maintain the HEMA partial pressure at 100 mTorr. Film growth was terminated at approximately 100 nm. For the graded co-polymer (experimental series G), HEMA was initially introduced into the reactor and the polymerization proceeded until approximately 80 nm of film was deposited. Then, PFM was introduced into the feed gas while the HEMA flow was kept constant, and the resulting co-polymer was deposited for an additional 20 nm of film deposition. The flow rates and pressures for both the bulk and graded co-polymers are summarized in Table 2.3.

Table 2.3. Experimental conditions for the co-polymer synthesis.

For the homogeneous films (series H), all the indicated flow-rates were used throughout the depositions. For the graded films (series G), no PFM was used at the start of the deposition.

Sample Name	HEMA Flow (sccm)	PFM Flow (sccm)	P _{total} (mTorr)	Molar composition (%PFM)
H0 & G0	2.0	0.0	100	0
H1 & G1	2.0	1.0	150	33
H2 & G2	2.0	3.0	250	60
H3 & G3	2.0	5.0	350	71

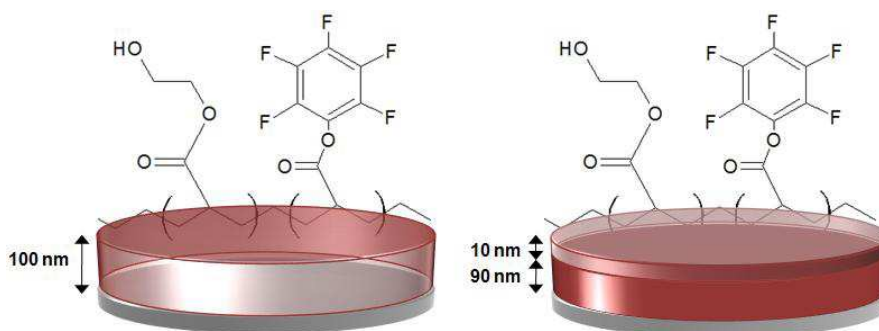


Figure 2.2. Schematic representation of the chemical composition and physical structure.

Bulk (left) and graded (right) co-polymer films.

2.2.3. Microsphere and Sensor Modification

Experimental condition B2 was used to deposit films of pHEMA on silica microspheres of diameter 50-100 μm (Polysciences), and monodisperse silica spheres of nominal diameter 5.0 μm (Bangslab) and 0.8 μm (Bangslab).

The 50-100 μm silica microspheres were carefully placed as a monolayer in order to avoid agglomerations in a Petri dish in the vacuum chamber. No drying process was necessary since the use of commercial dry microspheres. The petri dish was placed inside the reactor and the standard polymerization process was started. Every 100 nm of film growth, the reactor was opened and the microspheres were shaken manually. Once the polymerization achieved a coating thickness of approximately 1 micron, the petri dish was discharged and microspheres were collected for further characterization.

5.0 μm and 0.8 μm of silica spheres solution (10 μL) were pipetted from the microsphere solution and diluted in tetrahydrofuran to dehydrate the microsphere surface to avoid agglomerations. After mixing the solution, 10 μL was placed on a silicon wafer and dried overnight in a vacuum oven at 60 $^{\circ}\text{C}$. The wafer was placed inside the reactor and the standard polymerization process was started. Once the polymerization was done, the wafer was discharged.

In another experiment, manual rocking of particles during polymerization was also evaluated. In this case, particles were placed in a petri dish and the same procedure as in the silica particles was followed, the polymerization was stopped once the film thickness achieved.

The experimental condition B2 was also used to deposit 100 nm of pHEMA film onto a flat optode sensor, whose preparation has been described in 2.2.1. The as-prepared optode was coated without further modification. The responses of the coated and uncoated optodes were characterized via fluorometry (Dubach, Harjes & Clark 2007a; Dubach, Harjes & Clark 2007b).

2.2.4. Chemical Characterization of Films

The chemical structure of the piCVD films was determined by Fourier Transform Infrared Spectroscopy (FTIR spectroscopy (Nicolet Nexus 870ESP)). FT-IR stands for Fourier Transform InfraRed, the preferred method of infrared spectroscopy. In infrared spectroscopy, IR radiation is passed through a sample. Some of the infrared radiation is absorbed by the sample and some of it is passed through (transmitted). The resulting spectrum represents the molecular absorption and transmission, creating a molecular fingerprint of the sample. Like a fingerprint no two unique molecular structures produce the same infrared spectrum. This makes infrared spectroscopy useful for several types of analysis. Therefore, infrared spectroscopy can result in a positive identification (qualitative analysis) of every different kind of material.

The piCVD films were analyzed as deposited on the silicon wafers. To compare piCVD-synthesized pHEMA to conventional solution-synthesized pHEMA, a pHEMA standard (Aldrich) was spun-cast onto a silicon wafer from a 1.0 wt% solution in tetrahydrofuran. Spectra were gathered in transmission mode using a liquid N₂ cooled MCT detector at 4 cm⁻¹ resolution averaged over 256 scans. All spectra were baseline-corrected.

2.2.5. Swelling Characterization of Films

The film swelling capacity was determined via spectroscopic ellipsometry (M-2000, J. A. Woollam) measurements of thickness. Ellipsometry is a technique that measures changes in polarization as light reflects or transmits from a material structure. The polarization change is represented as an amplitude ratio, Ψ , and the phase difference, Δ . The measured response depends on optical properties and thickness of individual materials. Thus, ellipsometry is primarily used to determine film thickness and optical constants. However, it is also applied to characterize composition, crystallinity, roughness, doping concentration, and other material properties associated with a change in optical response.

The wafer was cut into 25 × 80 mm strips prior to measuring thickness. Dry film thicknesses were determined by spectroscopic ellipsometry at an incident angle of 75°. The data were fit to a Cauchy-Urbach isotropic model (WVASE 32, J. A. Woollam). The films were then mounted in a liquid cell (J. A. Woollam) and the cell was injected with a phosphate buffer solution at pH 7.4 (Cellgro, Mediatech). Ellipsometric data was then collected 1, 3, 5, 10, and 30 min post-injection of the buffer solution and fit to a Cauchy-Urbach isotropic model with an ambient water layer to determine the swollen thickness. In all cases, the film reached its equilibrium film thickness after 5 min. The water content of the swollen film was determined by dividing the increase in film thickness by the total thickness of the swollen film. This method of determining equilibrium swollen water content has been previously shown to closely match the more complex effective medium approximation (Chan & Gleason 2005b), where the swollen polymer is modeled as a composite layer of dry polymer and water. To test the stability of the polymer films and the reversibility of the swelling response, films were rinsed in

deionized water, dried in a vacuum oven overnight, and their dry and swollen thicknesses were determined again.

2.2.6. Interaction of pHEMA with Proteins

X-ray photoelectron spectroscopy (XPS) was used to quantify the degree of non-specific protein adhesion on the pHEMA films. X-ray photoelectron spectroscopy is a quantitative spectroscopic technique that measures the elemental composition, empirical formula, chemical state and electronic state of the elements that exist within a material. XPS spectra are obtained by irradiating a material with a beam of X-rays, while simultaneously measuring the kinetic energy and number of electrons that escape from the top 1 to 10 nm of the material being analyzed. XPS requires ultra-high vacuum conditions.

A 1 w/v % protein solution was prepared by dissolving 200 mg of bovine serum albumin (BSA, Fraction V, Sigma Aldrich) in a total volume of 20 mL of phosphate buffer solution. Three pieces of sample B2 and three pieces of a bare silicon wafer were incubated in the protein solution for three hours at 37 °C. Samples were then rinsed with approximately 5 mL buffer solution to remove loosely-bound protein and dried gently under nitrogen. The surface nitrogen content of each sample was then quantified by XPS (Kratos AXIS Ultra) survey scans, as an indicator of the amount of adsorbed protein.

2.2.7. Depth Profile of Films Determined by ToF-SIMS

Time-of-Flight Secondary Ion Mass Spectrometry (ToF-SIMS) uses a pulsed primary ion beam to desorb and ionize species from a sample surface. The resulting secondary ions are accelerated into a mass spectrometer, where they are mass analyzed by measuring their time-of-flight

from the sample surface to the detector. ToF-SIMS provides spectroscopy for characterization of chemical composition, imaging for determining the distribution of chemical species, and depth profiling for thin film characterization.

The ToF-SIMS analyses reported here were performed on a ToF-SIMS type ION-ToF IV instrument, equipped with Bi polyatomic primary ion source, a Cs/electron impact dual source column (DSC), and a low-energy electron flood gun (for charge compensation of insulating samples). The incidence angle of both the Bi and Cs ion sources was set at 45°. The operating analysis conditions were as follows.

Sputter etching of the surface was accomplished with a beam of 500 eV Cs⁺ ions (with a target current of 30 nA) rastered over a 400 mm x 400 mm area. A pulsed beam of 25 keV Bi³⁺ ions, scanned over a 100 mm x 100 mm region centered within the sputtered area, was used to generate secondary ions for analysis in negative ion mode.

A high current beam of low energy (<20 eV) electrons was employed for charge compensation. Mass resolution (m/Dm) was higher than 5000 and full spectra from 1 to 800-amu were acquired for all depths profiles. The signals were plotted once they were completely stabilized; the initial period was due to a transient effect until a sputtering steady state was reached. The surface oxidation also contributes to this effect modifying the ionization at the first film nanometers.

2.2.8. Surface Functionalization of Thin Film Hydrogels

Functionalization of the samples (G & H) was performed with a 0.05 M solution of O,O-bis (2-aminoethyl) polyethylene (PEG-diamine, Sigma) in ethanol ((100%) absolute, VWR). Hydrogels

were incubated in the PEG-diamine solution at 30 °C for 1 hour. Samples were then washed with ethanol to remove any unreacted ligand and dried with nitrogen at room temperature.

2.2.9. Silica Microspheres Coated with pHEMA

After coating with pHEMA, the silica microspheres were freeze-fractured and the particle cross-section was imaged using scanning electron microscopy (SEM, JEOL-5910). For silica microspheres, both uncoated and coated particles, were imaged (JEOL-6320FV) and their diameters measured via built-in image processing in the SEM software (JEOL Orion).

The SEM produces a largely magnified image by using electrons instead of light to form an image. A beam of electrons is produced at the top of the microscope by an electron gun. The electron beam follows a vertical path through the microscope, which is held within a vacuum. The beam travels through electromagnetic fields and lenses, which focus the beam down toward the sample. Once the beam hits the sample, electrons and X-rays are ejected from the sample. Detectors collect these X-rays, backscattered electrons, and secondary electrons and convert them into a signal that is sent to a screen similar to a television screen. This produces the final image.

2.3. Results

2.3.1. piCVD Deposition Mechanism and Chemical Structure OF pHEMA-based Hydrogels

In iCVD, a thermally labile initiator flows into the reactor along with a vinylic monomer. It is thought that iCVD proceeds by the reaction of vapor phase radicals, generated at hot filaments above the substrate, with surface adsorbed monomer (Baxamusa & Gleason 2008b). In contrast, in the piCVD process described here, HEMA is the only species introduced into the reactor; therefore, the polymerization must be initiated by the UV irradiation of HEMA monomers. Indeed, at UV wavelengths below 267 nm, carbonyl species are known to decompose into radicals (Abrahams et al. 1966) which in turn can initiate a free radical polymerization. Further research, beyond the scope of this current report, is required to determine whether this decomposition occurs in the vapor phase, at the surface, or in both locations, because the UV light reaches into contact with the vapor phase and the substrate. Surface radicals can react with the vinyl monomers present at the surface to initiate polymerization. Vapor phase radicals can either adsorb on the surface and subsequently react with adsorbed monomers or directly strike adsorbed monomers and react by an Eley-Rideal mechanism (Adamson & Gast 1997) to form a growing polymer chain. Since polymer growth can be monitored in real time at the surface of the substrate by laser interferometry, the thickness of the film can be accurately controlled.

In order to compare the chemical structure retention of piCVD films, the IR spectra of piCVD-obtained pHEMA and pHEMA polymer standards were compared. Figure 2.3. shows the FTIR spectra of a pHEMA film deposited on a silicon wafer via piCVD and a pHEMA standard spin-casted onto a silicon wafer. Despite the fact that the monomer itself decomposes into radical

species during piCVD, the resulting polymer film retains the vast majority of the pendant hydroxyl and carbonyl groups present in the monomer.

The absence of absorption signals due to unsaturated carbon at $1640 - 1660 \text{ cm}^{-1}$ or $3000 - 3100 \text{ cm}^{-1}$ indicates that monomer reacted through their vinyl moiety to form a polymer. Both the piCVD and the standard polymer exhibit a broad band at $3200 - 3600 \text{ cm}^{-1}$, corresponding to the hydroxyl group, and a sharp band and intense at $1725 - 1730 \text{ cm}^{-1}$, corresponding to carbonyl stretching (Lin-Vien et al. 1991). Therefore, these data demonstrate that the piCVD of HEMA monomer proceeds through a free-radical mechanism, while retaining the side-group functionality.

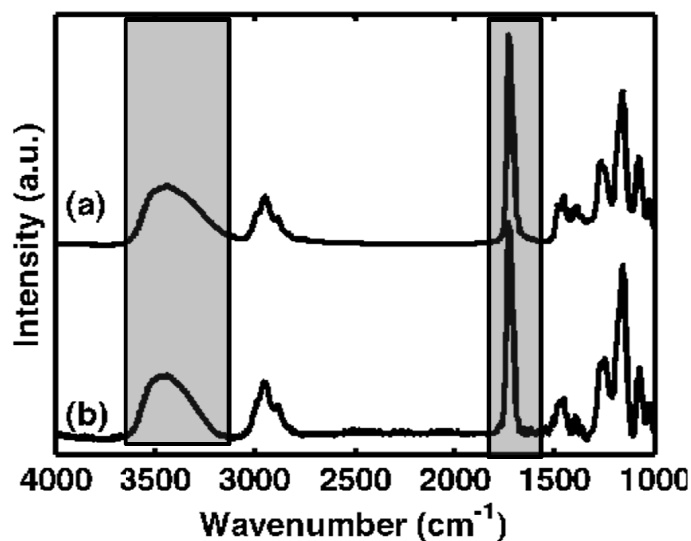


Figure 2.3. Comparison of FTIR spectra between pHEMA standard and piCVD synthesized.

FTIR spectra of (a) pHEMA standard and (b) piCVD-synthesized pHEMA. pHEMA standard was spin-casted on a silicon wafer from a 1% w/v solution in THF. piCVD pHEMA was obtained with a HEMA flow of 2 sccm to achieve a final film thickness of 100 nm.

In order to evaluate the retention of the chemical structure of piCVD films, both random and graded co-polymers prepared from PFM and HEMA were analyzed using IR spectroscopy.

Figure 2.4. shows the FTIR spectra of three bulk co-polymers and three graded co-polymers having the same PFM/HEMA ratios. A pHEMA film synthesized via piCVD is shown as a reference. The labeled mole percentages of HEMA and PFM represent the gas phase composition. In most cases, the gas composition differs from the expected values, reflecting the differences in the volatility of the two monomers and their reactivity ratios (Lau & Gleason 2006). The spectrum of the pure HEMA contains three main vibrational modes (Chan & Gleason 2005b). The most intense of these bands is found at $\sim 1725\text{ cm}^{-1}$ and corresponds with the C=O stretching. The C-H bending appears in its normal range of $1500 - 1350\text{ cm}^{-1}$. The band located at $\sim 1260\text{ cm}^{-1}$ corresponds to the stretching vibrational mode of C-O. The presence of PFM is indicated by three main absorption bands. The narrow, weak band that appears at 1774 cm^{-1} can be associated with the retention of the carbonyl group from the active ester. The fluorinated phenyl ring has a typical band at 1522 cm^{-1} that appears as a sharp and intense band in the spectrum. In addition, the C-F vibrations can also be observed at 1000 cm^{-1} . The PFM absorption signals in the FTIR spectra for the bulk co-polymer are clearly expressed for all the ratios. Lower signal intensity can be observed in the PFM bands of the graded co-polymers, when compared to the bulk co-polymers. This phenomenon is probably caused because PFM is only present near the surface of graded films, as opposed to bulk co-polymers, where the PFM is incorporated throughout the entire hydrogel matrix. As a result, the absorption of the PFM bands in the graded co-polymers is lower

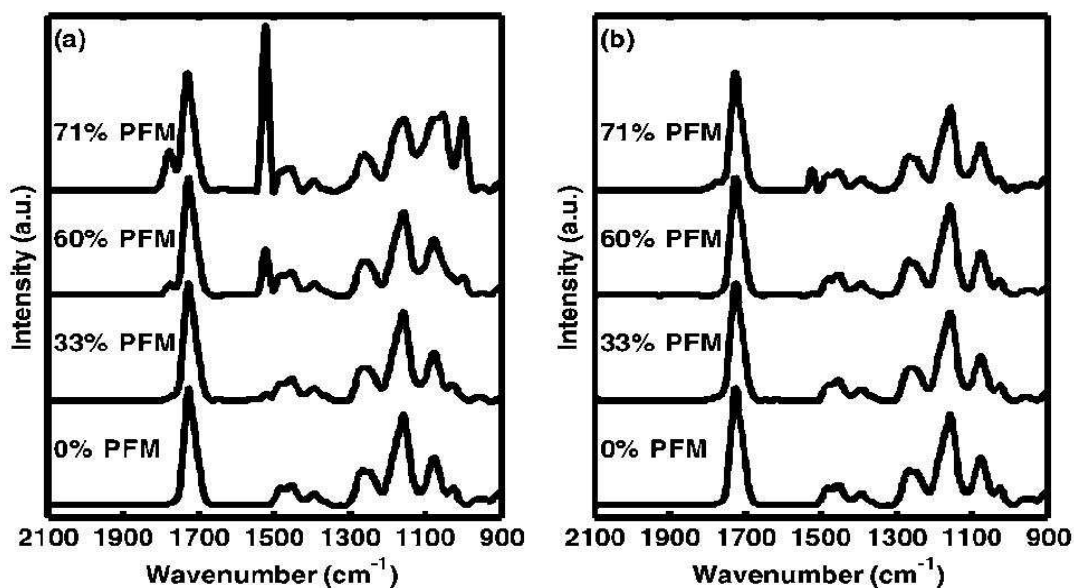


Figure 2.4. FTIR spectra of three co-polymer compositions.

(a) bulk co-polymers and (b) graded co-polymers, along with the spectra for pure pHEMA. The compositions refer to gas phase molar composition during piCVD synthesis.

2.3.2. Depth Profile of the PFM-functional Hydrogel

In order to confirm the gradual composition variation of the films, both bulk and graded co-polymers samples were analyzed using mass spectrometry depth-profiling studies. Depth profiles of positive ion ToF-SIMS spectra confirmed the film structure of the bulk and graded co-polymers. Figure 2.5. shows the intensity at $m/z = 253.1$, which corresponds to the charged PFM monomer fragment (M^{+1}) (Francesch 2008), as a function of film depth for both the bulk and graded co-polymers. The bulk co-polymer shows a relatively constant PFM content throughout the film depth. In contrast, the graded co-polymer shows the presence of PFM groups in the first 20 nm of film, confirming that the functionality in the graded co-polymer was nanoconfined to the near surface region.